POLYPUBLIE
Polytechnique Montréal

POLYTECHNIQUE MONTRÉAL
UNIVERSITÉ D'INGÉNIERIE

Titre: Title:	Influence of polypropylene fiber reinforcement on tensile behavior and failure mode of tailings cemented paste backfill
Auteurs: Authors:	Xin Chen, Xiuzhi Shi, Jian Zhou, & Zhi Yu
Date:	2019
Type:	Article de revue / Article
Référence: Citation:	Chen, X., Shi, X., Zhou, J., & Yu, Z. (2019). Influence of polypropylene fiber reinforcement on tensile behavior and failure mode of tailings cemented paste backfill. IEEE Access, 7, 69015-69026. https://doi.org/10.1109/access.2019.2919480

Document en libre accès dans PolyPublie
Open Access document in PolyPublie

URL de PolyPublie: PolyPublie URL:	https://publications.polymtl.ca/4820/
Version:	Version officielle de l'éditeur / Published version Révisé par les pairs / Refereed
Conditions d'utilisation: Terms of Use:	IEEE Open Access Publishing Agreement

Document publié chez l'éditeur officiel
Document issued by the official publisher

Titre de la revue: Journal Title:	IEEE Access (vol. 7)
Maison d'édition: Publisher:	IEEE
URL officiel: Official URL:	https://doi.org/10.1109/access.2019.2919480
Mention légale: Legal notice:	

Influence of Polypropylene Fiber Reinforcement on Tensile Behavior and Failure Mode of Tailings Cemented Paste Backfill

XIN CHEN[ID][1,2], **XIUZHI SHI**[1], **JIAN ZHOU**[ID][1], **AND ZHI YU**[1]

[1]School of Resources and Safety Engineering, Central South University, Changsha 410083, China
[2]Research Institute on Mines and Environment (RIME), Department of Civil, Geological and Mining Engineering, École Polytechnique de Montréal, Montréal, QC H3C 3A7, Canada

Corresponding authors: Xiuzhi Shi (shixiuzhi@263.net) and Jian Zhou (csujzhou@hotmail.com)

ABSTRACT Tailings were used to prepare cemented paste backfill (CPB) reinforced with polypropylene (PP) fiber, and fiber content and fiber length were 0-20 % and 3-12 mm, respectively. The Brazilian indirect tensile strength tests, macrostructural and microstructural (SEM) failure mode analyses and nuclear magnetic resonance (NMR) tests were performed. The results demonstrate that PP fiber with high tensile strength can substantially enhance the tensile strength and ductility of CPB specimens. The fiber-reinforced CPB exhibits superior performance during the pre-peak and post-peak stages and can retain its residual strength after being broken. The fiber-reinforced CPB provided a higher secant Young's modulus and strain at peak stress than that of the unreinforced CPB. From the failure mode analysis, fiber was used to bridge the CPB microelements and combine these effectively with calcium silicate hydrate gelling. The governing failure mode of fiber is pulled out or pull off, through which fiber absorbs the tensile stress and energy. However, fiber is also believed to have confusion distribution in CPB because fiber cannot reach their full strain capacity, especially at the later curing stage. And the weak structural layers in the CPB can also be formed, and the higher tensile strength is not achieved with the additional fiber content or longer fiber length. The optimal fiber content in this study is recommended to be 0.15 %, and it's better to choose 6 or 9 mm fiber. Moreover, fiber can reduce the original porosity by 10.72 %, but only has a slight influence on the pore size. The decrease in porosity helps increase the tensile strength of the fiber-reinforced CPB.

INDEX TERMS Tailings, fiber-reinforced, cemented paste backfill, Brazilian indirect tensile strength.

I. INTRODUCTION

Cement-based materials are used extensively worldwide in building and construction, and are also applied in mining engineering as cemented paste backfill (CPB), owing to its excellent compressive strength [1]–[5]. However, in usual cases, the tensile strength of a cement-based material is significantly lower than its compressive strength. Its poor tensile strength and strain capacity make the tensile failure to be one of the basic forms of cement-based-material failure and limit its applications [6]–[9]. Particularly for CPB in mining engineering, an increasing number of fine tailings need to be

The associate editor coordinating the review of this manuscript and approving it for publication was Bo Sun.

disposed of, because the ore is crushed into finer particles to improve mineral recovery [3], [10], [11]. However, as a result of its unreasonable gradation, tailings used in CPB preparation can easily lead to the low strength, especially the tensile strength [10], [12], Besides, sulfur tailings containing sulfide minerals or treated by sulfide cause acid attack to CPB matrix [13], [14]. Sulfate will promote secondary hydration products which can lead to the expansion, low strength and failure of CPB. Besides, CPB made of fine tailings has higher porosity than that of the ordinary CPB [13], and the research shows that high porosity will decrease the compressive strength in an exponential trend [15]. According to the research, CPB containing maple-wood filler with a relatively low porosity can improve the compressive strength [16].

Few studies are focused on the porosity related to tensile strength. Thus, improving the use of tailings to help improve the tensile strength of CPB remains an important research topic.

In order to overcome the shortcomings of cement-based materials, numerous studies have been carried out on mixing different types of fiber that have high tensile strength, excellent mechanical performance and engineering performance, such as steel, polypropylene, glass, and carbon fiber [17]–[21]. Various researchers have indicated that fiber-reinforced concrete exhibits superior mechanical properties [22]–[24]. With its wide dissemination throughout the construction industry, there has recently been increasing interest in the use of fiber in fiber-reinforced cemented sand and soil [25]–[32]. Polypropylene (PP) fiber can improve indirect tensile strength and stiffness [26]. And the post-peak behavior is also strongly affected by PP fiber content and length. The reinforcement of CPB with PP fiber demonstrated that fiber restrained the growth of crack by means of CT scans [33]. A great deal of work is required to study the tensile properties of cement-based materials, because conventional tests such as compressive and shear tests cannot precisely explain the crack phenomena [34]. The Brazilian test is widely accepted as an effective indirect tensile strength (ITS) test method to test the ITS of samples [35], [36]. It can overcome the special requirements of the direct tensile strength test for specimens and the study of the tensile strength characteristics of cement-based materials provides extensive benefits [37]. Therefore, significant work is still required on fiber-reinforced CPB, because the CPB properties differ from those of concrete, cement sand, soil, particularly in tailings CPB because of its poor backfill performance.

Therefore, in this project, Brazilian ITS experiments were carried out on tailings CPB to study the tensile behavior of CPB after adding PP fiber, including tensile strength (σ_{tB}), secant Young's modulus (E_{50}), and strain at peak stress (ε). Moreover, the crack development, porosity and structure change of the CPB failure mode were tested and analyzed by scanning electron microscopy (SEM) and Nuclear magnetic resonance (NMR).

II. MATERIALS AND METHODS
A. MATERIALS CHARACTERIZATION
Additional geotechnical, tailings particle size distribution and PP fiber properties have been reported refer to [38]. The following is the essential information presented in the aforementioned publication and some additions. The tailings were produced from mineral processing tailings by means of classification and concentration in the Fan Kou lead-zinc mine [39]. The particle size distribution of tailings were tested by LS particle size analyzer, and the results were shown in Fig. 1. With proportions of more than 47.15 % for particle sizes less than 20 μm diameter, the tailings were classified as medium [13]. Based on the geotechnical characterization
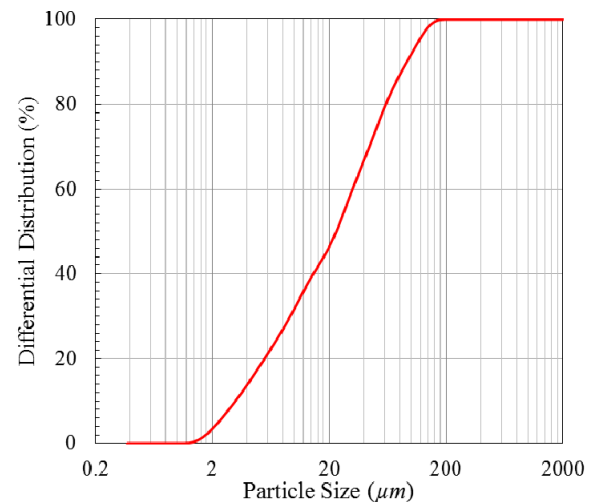

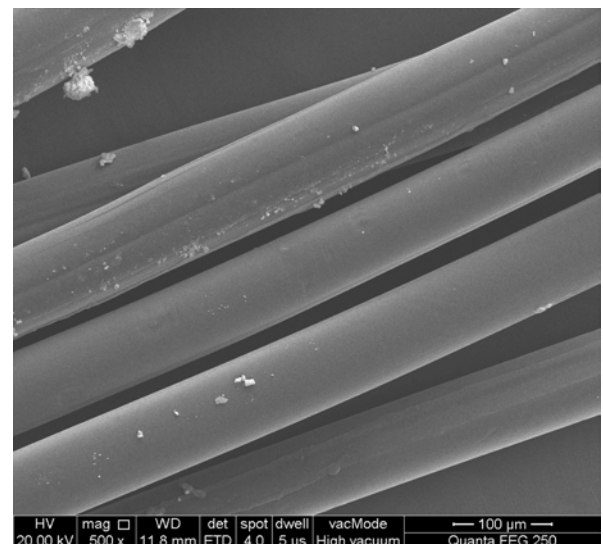**FIGURE 1.** The particle size distribution of the tailings.

FIGURE 2. The micro shapes of PP fiber.

of tailings, the tailings were similar to CL – lean clay [40]. By the XRF and XRD tests, the total content of main oxides amounted to 81.98 %, and pyrite are the main mineralogical compositions of the tailings. Additions, the sulfur content in tailings is 11.9 %.

Portland cement PO 42.5R was used as the binder in the CPB, and PP fiber was used to reinforce the CPB. Following mixing with tap water, fascicular PP fiber was dispersed into monofilament fiber, benefiting from the effective dispersion properties. The tensile strengths and elastic modulus values are all larger than 350 MPa and 3.5 GPa, respectively. The length of PP fiber used in this study is approximately 3 mm to 12 mm. In addition, the micro shapes of PP fiber is tested by SEM (Fig. 2).

B. SPECIMEN PREPARATION
The orthogonal table of L_{16} (4^4) was selected to implement the backfill tests [3], [38], as identified in Table 1.

TABLE 1. Orthogonal table L_{16} (4^4) of all mixtures fabricated.

Mixture	Cement content[a] (%)	Solid mass concentration[b] (%)	Fiber content[c] (%)	Fiber length (mm)
T1	A_1	B_1	C_1	D_1
T2	A_1	B_2	C_2	D_2
T3	A_1	B_3	C_3	D_3
T4	A_1	B_4	C_4	D_4
T5	A_2	B_1	C_2	D_3
T6	A_2	B_2	C_1	D_4
T7	A_2	B_3	C_4	D_1
T8	A_2	B_4	C_3	D_2
T9	A_3	B_1	C_3	D_4
T10	A_3	B_2	C_4	D_3
T11	A_3	B_3	C_1	D_2
T12	A_3	B_4	C_2	D_1
T13	A_4	B_1	C_4	D_2
T14	A_4	B_2	C_3	D_1
T15	A_4	B_3	C_2	D_4
T16	A_4	B_4	C_1	D_3

Note: [a] Relatively to the tailing weight.
[b] Solid mass include tailing + cement + fiber.
[c] Relatively to the tailing + cement weight.

FIGURE 3. CPB specimens: fiber-reinforced and unreinforced.

The material proportion of CPB mainly have 4 factors and 4 levels in this study, including cement content (A_1-A_4: 25-14 %), solid mass concentration (B_1-B_4: 60-66 %), fiber content (C_1-C_4: 0.05-0.20 %), and fiber length (D_1-D_4: 3-12 mm). The detailed preparation process and curing methods have been described in the previous publication [38]. The molds used to prepare the specimens for tensile strength test are different from the molds used for UCS tests. In this study, as shown in Fig. 3, the CPB samples were shaped by cylindrical plastic molds with a diameter of 50 mm diameter and a height of 50 mm.

The slump of fresh slurry was tested before the ITS test, and the slump of unreinforced backfill and fiber-reinforced backfill are 19.5–21.6 cm and 19.8–22.9 cm, respectively. The results indicated that the effect of adding fiber on the fluidity of fresh slurry is slight, and it can be transported by pumping methods [38].

C. ITS TESTS

Brazilian tests were used to overcome the shortcomings of direct tensile strength tests, including sample processing

difficulties and eccentricity existing during the loading process [37], [41], [42]. Because ITS tests can be conducted using conventional compressive test equipment, and 3 specimens per mixture were tested for each curing time. As illustrated in Fig. 4 [43], in the Brazilian ITS test, the specimens are placed between the machine plates, and the line load was formed in the interior of specimens by two hard steel strips.

D. FAILURE MODE ANALYSIS

During the development of tensile stress applied on the CPB specimens, the inner part of the CPB specimens began to get damaged, with micro-cracks forming and developing. Finally, forming through cracks, the specimens underwent tensile failure. Images recording the process of the ITS tests and crack features during the tests were analyzed to study the CPB macroscopic failure mode. The fiber distributions in the specimens could be clearly reflected.

E. MICROSTRUCTURE ANALYSIS

The microscopic materials composition, the contact modes between fiber and CPB matrix and the failure modes of fiber were tested with SEM [16]. SEM is also useful to analyze the force of CPB microelements.

The pore structure of the CPB specimens was tested by NMR method. T_2 distribution of transverse relaxation time is the key index to evaluate the pore structure of CPB, and it can be referred to Equation (1). Therefore, the change of T_2 spectrum can reflect the distribution and size of the pores in CPB [11].

$$\frac{1}{T_2} = \rho_2 \left(\frac{S}{V}\right)_{pore} \tag{1}$$

where T_2 is the transverse relaxation time, ms; ρ_2 is the transverse surface relaxation strength, μm/ms; and S/V is the ratio of the surface area to the volume of pore.

III. RESULTS AND DISCUSSION
A. INFLUENCE OF FIBER ON INDIRECT TENSILE BEHAVIOR

In order to predict the tensile stress distribution in specimen theoretically, it's assumed that the mechanical behaves of CPB elastically during both the tensile and compressive processes, and the stress distribution at the specimen center is unaffected by the loading damaged zone, and crack initiation occurs at the center. As suggested by the classical theory of the International Society for Rock Mechanics (ISRM) [37], the Brazilian ITS (σ_{tB}) of CPB can be calculated using Equation (2) [37], [44].

$$\sigma_{tB} = -2P/\pi dt \tag{2}$$

where P is the applied vertical load, d is the CPB disc specimen diameter, and t is the CPB disc specimen thickness.

As show in Fig. 4, the surface load is converted into line load and compressed on the CPB by the action of the experimental device. Assume that the CPB is a homogeneous
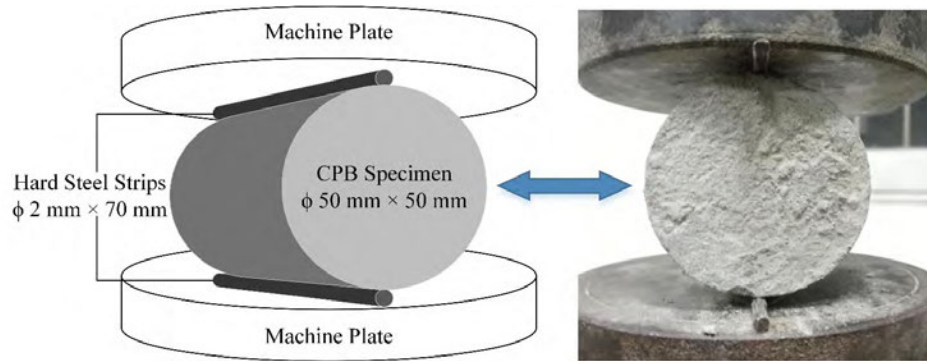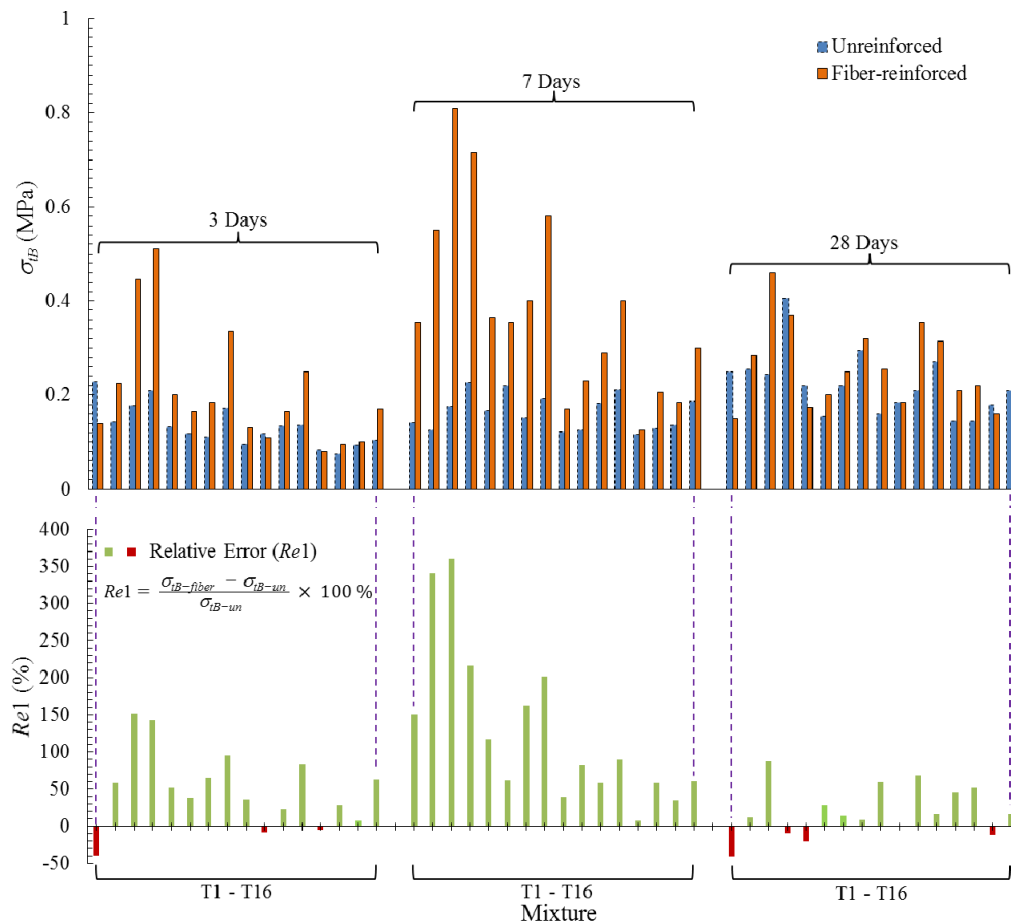
FIGURE 4. ITS test setup [43].

FIGURE 5. ITS of fiber-reinforced and unreinforced and their *Re1* with different curing times.

material and the upper and bottom contact angles of the CPB and the experimental device are the same, tensile stress and compressive stress maximize at the center of the CPB, which cause the initiate crack at the same position. Studies have shown that the strength ratio of compressive to tensile of the materials is 3 under those conditions, and this ratio of CPB is 10-20 [37]. Therefore, splitting failure of the CPB which is a kind of low strength cement-based material in Brazilian

ITS test, and Equation (2) can be used to express the tensile strength of the CPB.

The results of the Brazilian ITS tests and relative error between the fiber-reinforced and unreinforced tensile strength are presented in Fig. 5. The addition of PP fiber improves the ITS of CPB significantly. More than 80% of the mixture fiber-reinforced specimens exhibited increased tensile strength. The mixture T3 exhibited that the tensile
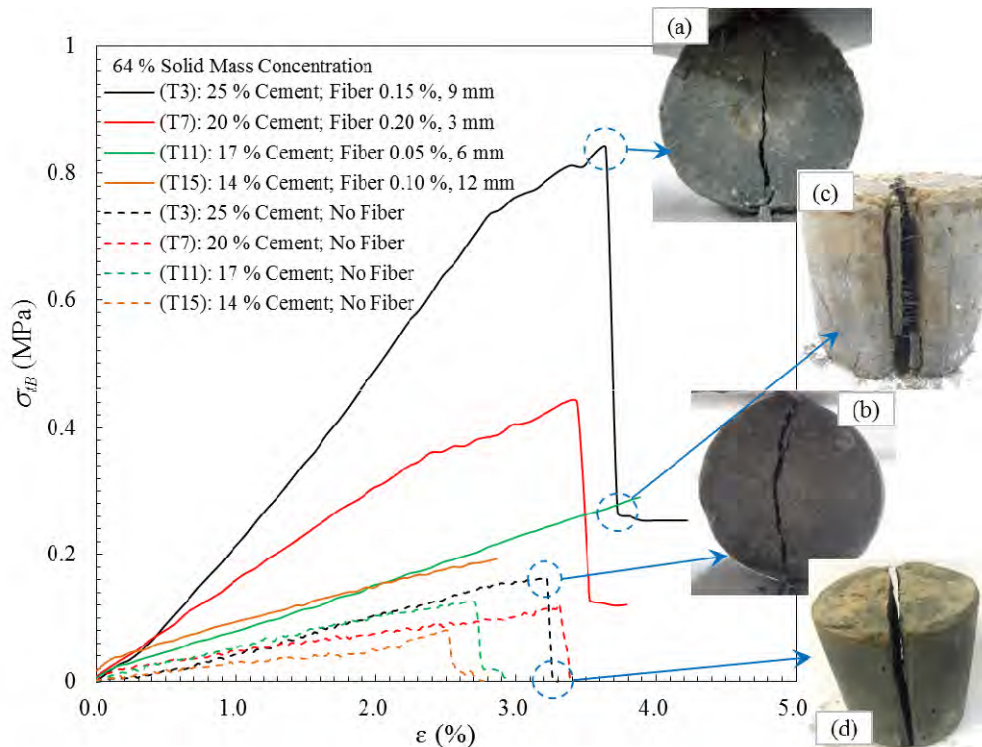
FIGURE 6. Tensile stress-strain curves of fiber-reinforced and unreinforced CPB.

TABLE 2. Secant Young's modulus and strain at peak stress of the corresponding curves in Fig. 6.

Mixture	Secant Young's Modulus/E_{50} (MPa)			Strain at Peak Stress/ε (%)		
	Fiber-reinforced	Unreinforced	$Re2^{a}$ (%)	Fiber-reinforced	Unreinforced	$Re3^{b}$ (%)
T3	24.90	5.28	371.59	3.64	3.21	13.40
T7	15.46	4.00	286.50	3.43	3.32	3.31
T11	6.48	5.91	9.64	3.88	2.72	42.65
T15	6.17	2.80	120.36	2.85	2.51	13.55

Note: [a] $Re2 = (E_{50-fiber} - E_{50-un})/E_{50-un} \times 100\,\%$

[b] $Re3 = (\varepsilon_{fiber} - \varepsilon_{un})/\varepsilon_{un} \times 100\,\%$

strength of the fiber-reinforced CPB can increase maximum by 360 % than that of the unreinforced specimens at 7 days of curing. These demonstrate that, with the addition of the PP fiber, the CPB specimens can resist higher tensile loads. Furthermore, Fig. 5 indicates that cementitious binder with strong bonding properties can provide a cohesive force against the imposed tensile stress, and high concentration can improve the stability of CPB after consolidation [45].

In this study, the tensile strength of unreinforced CPB exhibits a significant decrease when compared to the tensile strength of the fiber-reinforced CPB at 28 days of curing. Two reasons are presented as following:

1) The CPB matrix exhibits significantly higher ductility during the early stages, and the friction between the viscous cement matrix and fiber is stronger, which is beneficial to the fiber enhancement. At the later curing stage, some of the fiber will be pulled off and pulled out with the development of cracks in the CPB matrix, which lead to those fiber cannot fully exert the tensile effect.

2) There is 11.9 % sulfate in the tailings forming the secondary products (gypsum and ettringite) that have expansibility Cwhich leads to the generation of cracks inside of CPB, and the final failure of CPB. Therefore, tensile strength was improved at the beginning of curing, but decreased at the 28 days curing time.

Fig. 6 depicts the tensile stress-strain curves of the fiber-reinforced and unreinforced CPB obtained during the Brazilian ITS tests. Prior to reaching the peak stress, all the specimens experienced obvious elastic or elastic-plastic deformation [46], [47]. Thereafter, the specimens underwent fracture failure under the load higher than ultimate tensile strength. The addition of fiber can increase the peak tensile strength, and corresponding strain and secant Young's modulus (E_{50}) (Table 2). The increase of E_{50} of the fiber-reinforced CPB is significant except for T11 ($Re2 = 9.64\,\%$), while the E_{50} values of mixtures T3, T11, and T15 are more than twice those of the unreinforced CPB. Moreover, the peak stress strain also increased, and the highest strain growth ratio of

TABLE 3. Orthogonal range results of the ITS of fiber-reinforced CPB.

Curing Age	Range	A (MPa)	B (MPa)	C (MPa)	D (MPa)
3 Days	k_1	0.333	0.138	0.163	0.170
	k_2	0.225	0.152	0.195	0.205
	k_3	0.165	0.228	0.255	0.233
	k_4	0.113	0.305	0.222	0.228
	R_j	0.220	0.167	0.092	0.063
	Significance	A > B > C > D			
7 Days	k_1	0.610	0.258	0.328	0.343
	k_2	0.427	0.338	0.378	0.387
	k_3	0.272	0.422	0.443	0.428
	k_4	0.208	0.500	0.370	0.360
	R_j	0.402	0.242	0.115	0.085
	Significance	A > B > C > D			
28 Days	k_1	0.318	0.200	0.240	0.235
	k_2	0.237	0.225	0.238	0.295
	k_3	0.283	0.307	0.315	0.270
	k_4	0.210	0.315	0.255	0.248
	R_j	0.210	0.115	0.077	0.060
	Significance	A > B > C > D			

Note: k_i represents the average of UCS under level i
R_j represents the range of the difference between the max and min average values

mixture T11 was 42.65 %. All these positive effects of fiber on mechanical properties (σ_{tB}, E_{50}, and ε) in the pre-peak stage illustrate that fiber has a positive effect on the tensile properties of CPB. Furthermore, the fiber-reinforced CPB with greater values of E_{50} and ε exhibits a superior ability to resist the elastic deformation and displacement, which means that fiber-reinforced CPB exhibits higher stiffness and ductility than that of the unreinforced CPB.

Fiber can also enhance the post-peak strength and ductility of CPB. Fig. 6 (a) and (b) indicated that the crack width decreased with the addition of PP fiber when reaching the peak stress. The transfixion crack on the unreinforced CPB indicated that the matrix experienced fracture failure and completely lost its bearing capacity. And the strength dropped to 0 MPa (Fig. 6 (d)), which also illustrates this viewpoint. In contrast, the fiber-reinforced CPB was not completely broken and retained a certain residual strength, which provides a certain pressure-bearing capacity of CPB during failure. This is because of the intact structure that fiber provides, and the decrease in the CPB brittleness because of its strong fracture-resisting strength ability. As indicated in image (c) in Fig. 6, a large number of fiber, uniformly distributed in the CPB matrix, were pulled out or broken during the CPB matrix fracture failure. The ductility improvement also benefited from the fiber absorbing the tensile stress during the fiber pull out or pull off process, which is described in publication refer to [25].

B. INFLUENCES OF CEMENT, TAILINGS AND FIBER

As shown in Table 3, based on the orthogonal range analysis principle [48]–[50], the importance weight ranking of the influential factors is: A > B > C > D. As illustrated in Fig. 7 (a) and (b), the tensile strength basically increased monotonously with an increase in cement content and solid mass concentration. In many cases, fiber-reinforced CPB
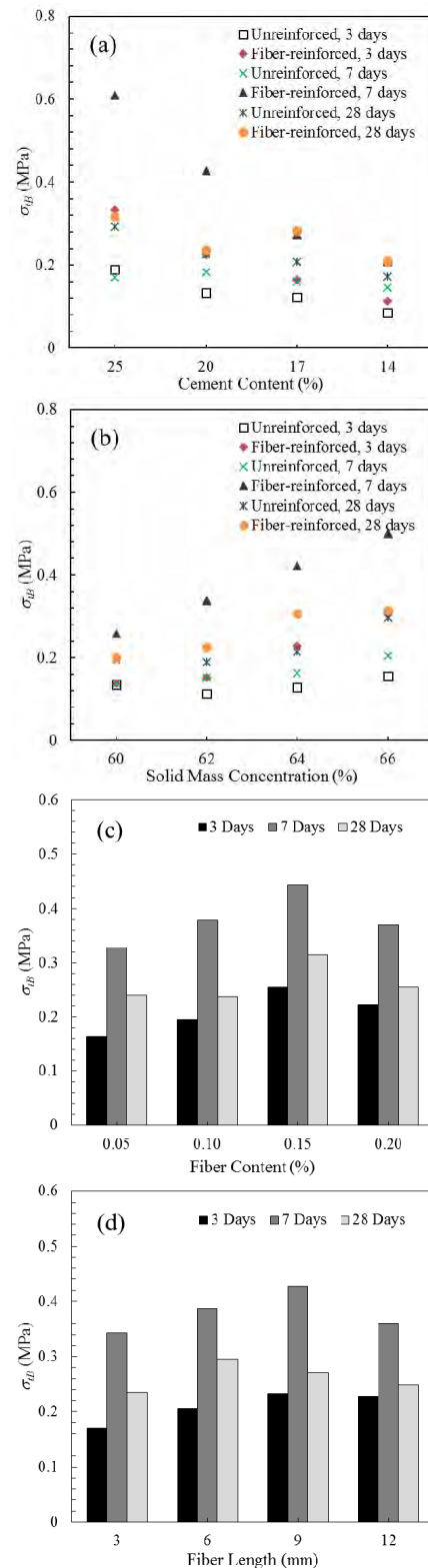
FIGURE 7. The influences of cement content (a), solid mass concentration (b), fiber content (c) and length (d) on average ITS.

with a low cement content could achieve the same strength level as unreinforced CPB with a high cement content. At 28 curing days, the tensile strength of the fiber-reinforced

TABLE 4. Tensile strength induced by PP fiber.

PP fiber tensile strength (MPa)	Fiber content (%)	χ (%)	t_t (MPa)	σ_{tB} at 7 days curing time (MPa)
350	0.05	0.11	0.385	0.328
	0.10	0.22	0.770	0.378
	0.15	0.33	1.155	0.443
	0.20	0.44	1.540	0.370

CPB with a cement content of 17 % is 0.283 MPa, which is higher than the tensile strength of the unreinforced CPB, at 0.225 MPa with a cement content of 20 %. Therefore, fiber-reinforced CPB can be used as a type of energy saving in backfill materials with low cement consumption.

The correlations between the tensile strength σ_{tB} and fiber at each curing time are illustrated in Fig. 7 (c) and (d). As the fiber content increased from 0.05 % to 0.20 %, the tensile strength first increased and then decreased. The relationship between ITS and fiber was not monotonic linear, and the tensile strength reached the maximum peaks when the fiber content was 0.15 %.

This is a consequence of the fact that the tensile strength doesn't always increase with increasing the fiber content. This conclusion can play an important guiding role in the improved fiber reinforcement effect and superior fiber cost control. At different curing times, the tensile strength first increases and then decreases with increasing the fiber length. When curing 3 and 7 days, the maximum tensile strength of the specimen occurred when the 9 mm fiber was added. However, after 28 days, when the fiber length was 6 mm, it was more helpful in improving the tensile strength.

To summarize, the better fiber parameters of fiber content of 0.15 % and fiber length of 6 or 9 mm can be obtained. Those conclusions can be explained as following:

1) Firstly, PP fiber can be effectively combined with the CPB matrix. A certain content and length of fiber acts as the bridge among the CPB matrix microstructures.

This effectively controls the crack development and enables the fiber-reinforced CPB to endure a higher peak tensile load.

2) However, weak structural layers are formed, combined with the fiber and hydrated products during the cement hydration reaction. Prior to the destruction of the cement matrix, the CPB will first be broken along the weak structural layers.

3) Furthermore, with the certain fiber content and density, longer fiber length and fewer quantity of fiber will lead to nonuniform distribution of fiber in the CPB matrix and weaken the fiber reinforcement effect. In summary, an optimal value exists for the fiber content and length.

In previous study, fiber was considered to provide final tensile stress after CPB matrix failure, and Equation (3) was proposed to estimate the tensile strength provided by fiber [51]. The tensile strength provided by PP fiber was shown in Table 4. Comparing with the ITS of CPB when curing 7 days, the t_t value is higher than the σ_{tB} value, which means that the CPB is not taking full advantage of the tensile strength of PP fiber. This is due to the confusion distribution of fiber in the CPB matrix, and the direction of fiber is not uniform. As shown in Fig. 8 and Fig. 9, some fiber was only pulled out but not pulled off, those fiber not reaching their full strain capacity. Moreover, too many fiber will lead to the generation of some weak structural planes in the CPB, and can also reduce the strength of CPB.

$$t_t = \chi \cdot \sigma_{f,ult} \qquad (3)$$

where t_t is the tensile strength induced by fiber; χ is the fiber volume content; $\sigma_{f,ult}$ is the ultimate tensile strength of an individual fiber.

Fig. 8 illustrates the macrostructural failure mode of CPB with different fiber contents and lengths. The unreinforced CPB specimens underwent complete brittleness failure to bear the external load. As illustrated in Fig. 8 (a), the specimen was divided into two parts along the fracture surface. In contrast, the fiber-reinforced CPB retained a residual strength and maintained its integrity with the effect of fiber. From Fig. 8 (b), (c), (d), and (e), the CPB ductility was
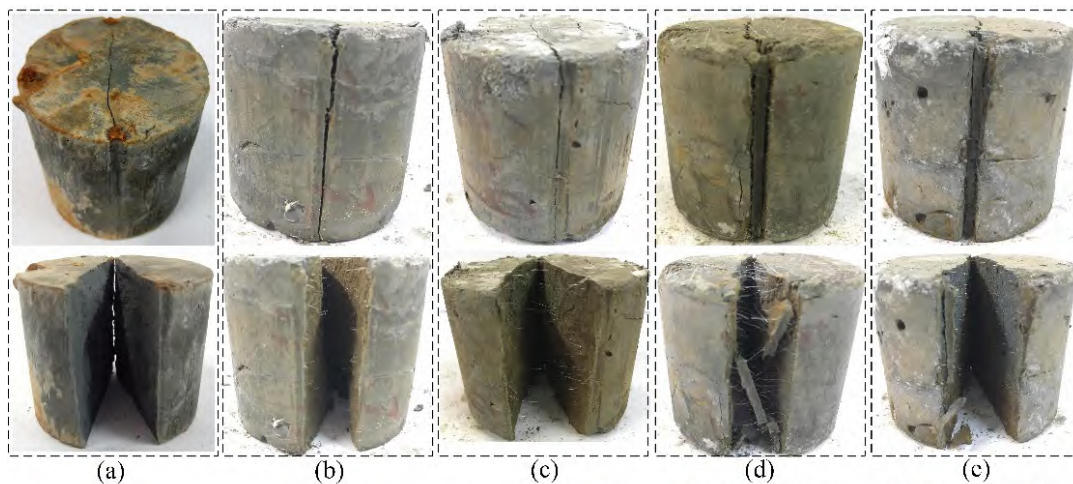

(a)   (b)   (c)   (d)   (e)

FIGURE 8. Macrostructural failure mode of CPB specimens with different content and fiber length. (a) No fiber.(b) PP fiber: 0.05%, 6 mm. (c) PP fiber: 0.10%, 12 mm. (d) PP fiber: 0.15%, 9 mm. (e) PP fiber: 0.20%, 3 mm.
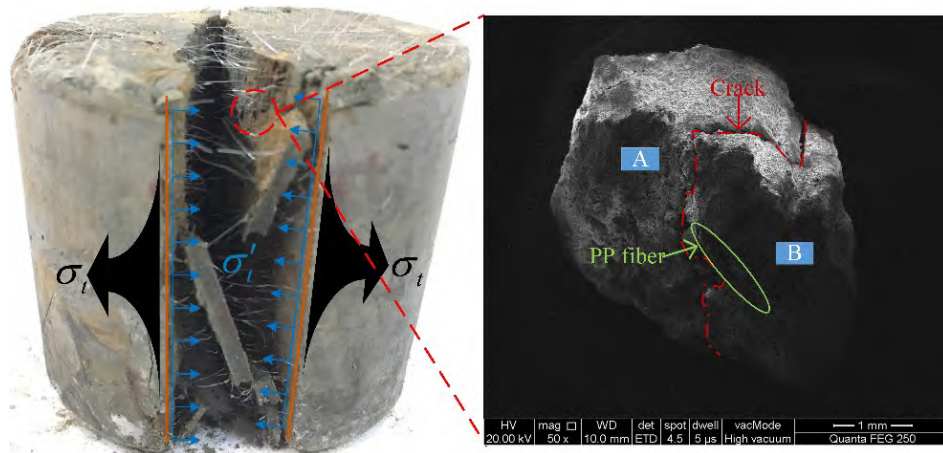
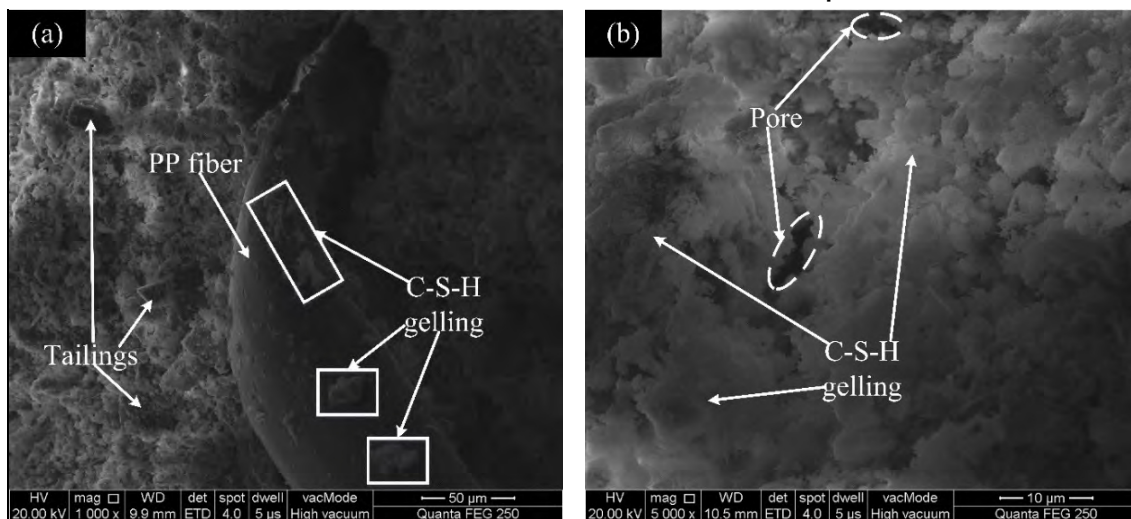**FIGURE 9.** Stress distribution and microelement structure of fiber-reinforced CPB specimen.

FIGURE 10. SEM micrographs of fiber-reinforced CPB specimen in different precision level. (a) 50 μm. (b) 10 μm.

significantly enhanced, and the fiber was widely distributed in the CPB interior and also on the fracture surfaces. Every fiber monofilament could use its fracture-resisting ability to counteract the CPB tensile stress in the interior generated by external loads, and also tended to bridge these cracks and prevented crack propagation, as illustrated in Fig. 8 (b) and (c) in particular. Therefore, the fiber reduced the crack numbers and widths, and reinforced the CPB tensile strength and ductility. It is worth mentioning that, because the fiber-reinforced CPB specimens still maintained an integrative structure after ITS tests, the researchers had to divide the specimens by hand to capture the images. Furthermore, the processing was it was more difficult to process the specimens with more or longer fiber transverse distribution, which also reflected the fact that fiber can reinforce both strength and ductility.

C. SEM RESULTS

As illustrated in Fig. 9, during Brazilian ITS tests, two outward tensile stresses (σ_t) from the center line of the specimen were generated inside the specimen under the external loads.
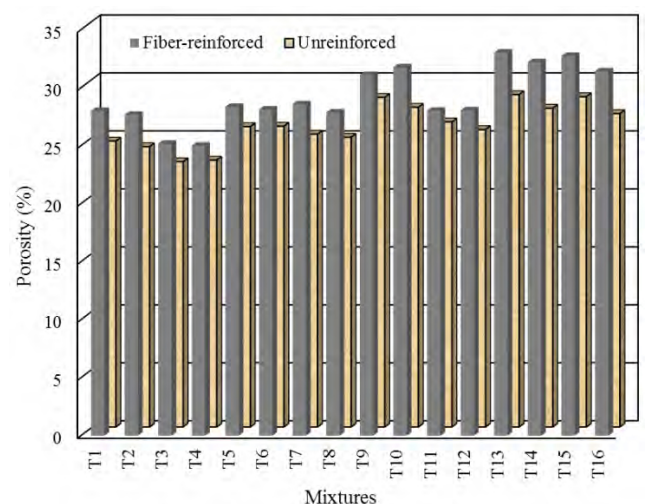

**FIGURE 11.** Porosity of fiber-reinforced CPB and unreinforced CPB.

Meanwhile, an opposite reaction (σ_t'), composed of cohesive stress among the CPB microelements and tensile stress provided by the fiber (if it was added), was generated to prevent

TABLE 5. The difference of porosity between unreinforced CPB and fiber-reinforced CPB.

| Mixture | Porosity (%) | | $Re4^a$ (%) | Mixture | Porosity (%) | | $Re4^a$ (%) |
	Unreinforced	Fiber-reinforced			Unreinforced	Fiber-reinforced	
T1	28.00	24.66	11.95	T9	31.10	28.42	8.60
T2	27.67	24.17	12.63	T10	31.77	27.57	13.21
T3	25.18	22.87	9.15	T11	28.02	26.30	6.11
T4	25.01	23.01	7.97	T12	28.06	25.65	8.58
T5	28.35	25.90	8.66	T13	33.03	28.66	13.23
T6	28.12	25.93	7.78	T14	32.20	27.49	14.65
T7	28.58	25.25	11.65	T15	32.74	28.48	13.00
T8	27.87	24.98	10.36	T16	31.42	27.02	13.99

Note: $Re4_{ave} = 10.72$ %

[a] $Re4 = \dfrac{n_{no-fiber} - n_{fiber}}{n_{no-fiber}} \times 100\%$, n represents the porosity.
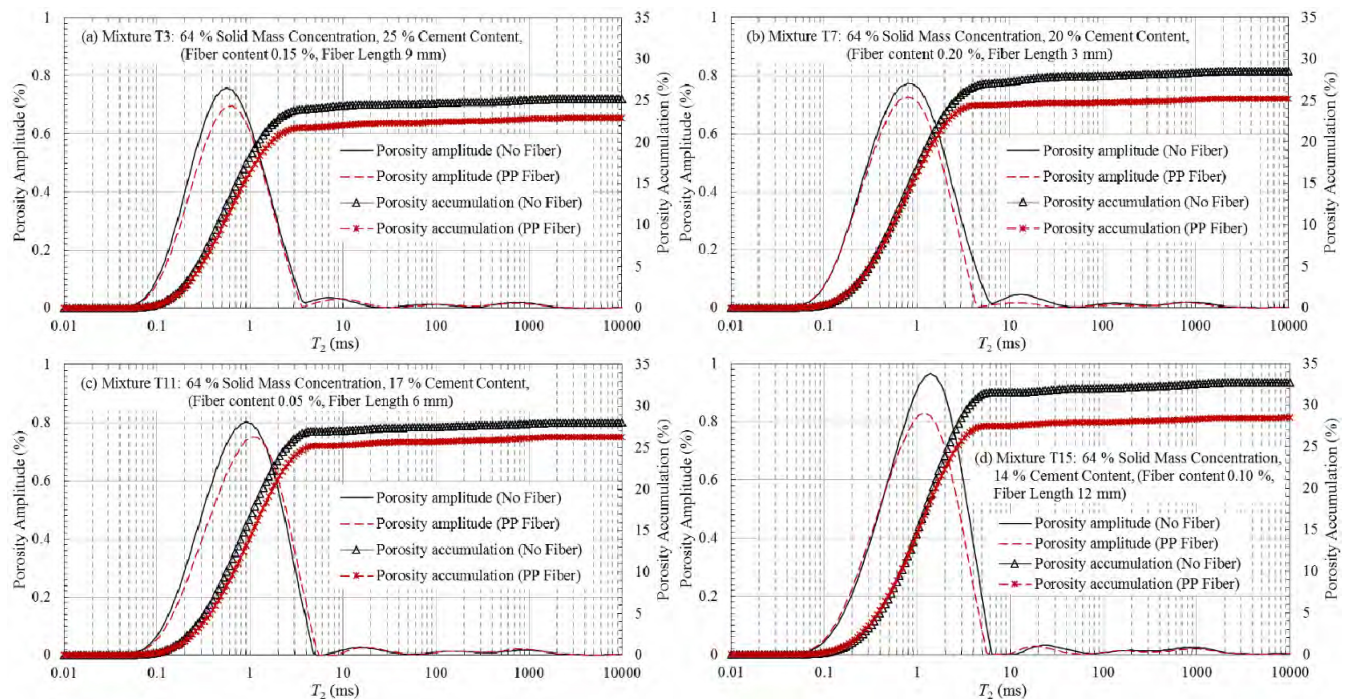
FIGURE 12. T_2 distribution of CPB at 28 days curing time with solid mass concentration 64%.

the σ_t from breaking the specimens. However, after the specimens experienced fracture failure, only the fiber tensile stress could support the opposite reaction to CPB. The connection relationship between the CPB and fiber was determined with SEM technology (Fig. 9), and the stress relation between these was clarified. SEM micrographs illustrates one piece of one fiber-reinforced CPB specimen. It is obvious that two separated parts A and B were still bridged by PP fiber as a result of the σ_t effect.

The SEM depicting the fiber-reinforced CPB specimens at 50 μm and 10 μm are provided in Fig. 10. These images demonstrated that a significant amount of calcium silicate hydrate (C-S-H, chemical formula: mCaO $\cdot$SiO$_2 \cdot$nH$_2$O) gelling was generated by the hydration reaction which provided load-bearing capacity [52]. Fig. 10 provides clear views of the contacting schemes among the particles,

C-S-H gelling, and PP fiber, indicating that all of them formed a whole structure. In the part of fiber that was pulled out, a certain amount of C-S-H remained trapped on the fiber surface. It can be seen that there were significantly more cloud C-S-H productions in the fiber-reinforced CPB specimens.

D. NMR RESULTS
Fig. 11 and Table 5 present the results of the NMR analysis, the porosity of unreinforced CPB ranges from 25.01 % to 33.03 %, and the porosity of fiber-reinforced CPB ranges from 23.01 % to 28.66 %. It is noteworthy that the CPB reinforced by PP fiber shows smaller porosity than that of the unreinforced CPB. PP fiber helps to enhance the compactness of CPB matrix, which is in a good agreement with the ITS results. In this study, PP fiber can reduce the original porosity

by 10.72 %, as shown in Table 5. In addition, the porosity decreases with the increase of solid mass concentration, but keeps increasing as the cement content decreases from 25 % to 14 %.

The results indicate that the increased cement content can lead to the generation of additional hydration products, which can fill the voids among tailings aggregates. Increasing solid mass concentration is also an effective way to decrease the porosity. This is because increasing the solid mass concentration means reducing the water content of CPB. When water is used or evaporated, a relatively few voids are formed.

Fig. 12 shows the T_2 distribution of CPB at 28 days curing time with solid mass concentration 64%. It is also proved that increasing the cement content and adding PP fiber can decrease the porosity of CPB. The change of T_2 spectrum can qualitatively describe the pores structure in CPB, and the pore size increases with T_2. Beside, fiber has only a slight influence on the pore size. It can be seen that the T_2 distribution curves of CPB are presented by the single wave peak images, and exhibit the same outlines between the unreinforced CPB and the fiber-reinforced CPB when the main wave peak ranges from 0.06ms to 5.94 ms.

IV. CONCLUSIONS

The ITS response and failure mode of tailings cemented paste backfill with PP fiber were analyzed and presented in this paper. Based on the Brazilian ITS tests, and the characterization of the macrostructure and microstructure, the main results of this study can be summarized as follows:

1) PP fiber with high tensile strength could substantially enhance the tensile strength, stiffness and ductility of the CPB specimens. Furthermore, the tensile stress-strain curves demonstrate that fiber could enhance the CPB tensile properties during both the pre-peak and post-peak stages.

2) The fiber-reinforced CPB retained residual strength after being broken, and its higher secant Young's modulus and strain at the peak stress helped to improve its ability to endure larger loads, elastic deformation and displacement.

3) The confusion distribution of fiber in CPB due to not all fiber not reaching their full strain capacity. The governing failure modes of fiber are pull out or pull off, through which fiber absorbs the tensile stress and energy.

4) The addition of fiber can reduce the porosity of CPB, but do not have significant influence on the pore size.

Moreover, the addition of PP fiber could help to reduce the financial cost by means of decreasing the cement cost. Future work could focus on the study on the effect of the wider ranges of fiber content and length on the behavior of CPB.
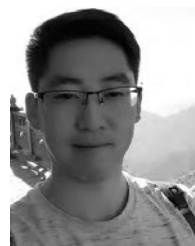
ACKNOWLEDGMENT

REFERENCES

[1] S. Kaliyavaradhan, T.-C. Ling, M.-Z. Guo, and K. H. Mo, "Waste resources recycling in controlled low-strength material (CLSM): A critical review on plastic properties," *J. Manage.*, vol. 241, pp. 383–396, Jul. 2019.

[2] Q.-S. Chen, Q.-L. Zhang, A. Fourie, X. Chen, and C.-C. Qi, "Experimental investigation on the strength characteristics of cement paste backfill in a similar stope model and its mechanism," *Construct. Building Mater.*, vol. 154, pp. 34–43, Nov. 2017.

[3] X. Chen, X. Shi, J. Zhou, Q. Chen, and C. Yang, "Feasibility of recycling ultrafine leaching residue by backfill: Experimental and CFD approaches," *Minerals*, vol. 7, no. 4, p. 54, Apr. 2017.

[4] X. Chen, J. Zhou, Q. Chen, X. Shi, and Y. Gou, "CFD simulation of pipeline transport properties of mine tailings three-phase foam slurry backfill," *Minerals*, vol. 7, no. 8, p. 149, Aug. 2017.

[5] L. Liu, Z. Fang, C. Qi, B. Zhang, L. Guo, and K. I.-I. L. Song, "Numerical study on the pipe flow characteristics of the cemented paste backfill slurry considering hydration effects," *Powder Technol.*, vol. 343, pp. 454–464, Feb. 2019.

[6] Z. Pan, L. He, L. Qiu, A. Korayem, G. Li, J. Zhu, F. Collins, D. Li, W. Duan, and M. Wang, "Mechanical properties and microstructure of a graphene oxide–cement composite," *Cement Concrete Compos.*, vol. 58, pp. 140–147, Apr. 2015.

[7] D. Kang, K. S. Seo, H. Lee, and W. Chung, "Experimental study on mechanical strength of GO-cement composites," *Construct. Building Mater.*, vol. 131, pp. 303–308, Jan. 2017.

[8] T.-C. Ling, S. K. Kaliyavaradhan, and C. S. Poon, "Global perspective on application of controlled low-strength material (CLSM) for trench backfilling—An overview," *Constr. Build. Mater.*, vol. 158, pp. 535–548, Jan. 2018.

[9] A. Mahdiyar, D. J. Armaghani, A. Marto, M. Nilashi, and S. Ismail, "Rock tensile strength prediction using empirical and soft computing approaches," in *Bulletin of Engineering Geology and the Environment*. Berlin, Germany: Springer, 2018, pp. 1–13.

[10] D. Q. Deng, L. Liu, Z. L. Yao, K. I. -I. L. Song, and D. Z. Lao, "A practice of ultra-fine tailings disposal as filling material in a gold mine," *J. Environ. Manage.*, vol. 196, pp. 100–109, Jul. 2017.

[11] J.-L. Li, K.-P. Zhou, W.-J. Liu, and H.-W. Deng, "NMR research on deterioration characteristics of microscopic structure of sandstones in freeze–thaw cycles," *Trans. Nonferrous Met. Soc. China*, vol. 26, no. 11, pp. 2997–3003, Nov. 2016.

[12] Q. Chen, Q. Zhang, C. Qi, A. Fourie, and C. Xiao, "Recycling phosphogypsum and construction demolition waste for cemented paste backfill and its environmental impact," *J. Clean. Prod.*, vol. 186, pp. 418–429, Jun. 2018.

[13] B. Ercikdi, H. Baki, and M. zki, "Effect of desliming of sulphide-rich mill tailings on the long-term strength of cemented paste backfill," *J. Environ. Manage.*, vol. 115, pp. 5–13, Jan. 2013.

[14] T. Yilmaz, B. Ercikdi, and H. Deveci, "Utilisation of construction and demolition waste as cemented paste backfill material for underground mine openings," *J. Environ. Manage.*, vol. 222, pp. 250–259, Sep. 2018.

[15] L. Liu, Z. Fang, C. Qi, B. Zhang, L. Guo, and K. I.-I. L. Song, "Experimental investigation on the relationship between pore characteristics and unconfined compressive strength of cemented paste backfill," *Construct. Building Mater.*, vol. 179, pp. 254–264, Aug. 2018.

[16] B. Koohestani, A. Koubaa, T. Belem, B. Bussiére, and H. Bouzahzah, "Experimental investigation of mechanical and microstructural properties of cemented paste backfill containing maple-wood filler," *Construct. Building Mater.*, vol. 121, pp. 222–228, Sep. 2016.

[17] S. Jiang, Q. Li, Y. Zhao, J. Wang, and M. Kang, "Effect of surface silanization of carbon fiber on mechanical properties of carbon fiber reinforced polyurethane composites," *Compos. Sci. Technol.*, vol. 110, pp. 87–94, Apr. 2015.

[18] C. Unterweger, J. Duchoslav, D. Stifter, and C. Fürst, "Characterization of carbon fiber surfaces and their impact on the mechanical properties of short carbon fiber reinforced polypropylene composites," *Compos. Sci. Technol.*, vol. 108, pp. 41–47, Feb. 2015.

[19] C. X. Qian and P. Stroeven, "Development of hybrid polypropylene-steel fibre-reinforced concrete," *Cement Concrete Res.*, vol. 30, no. 1, pp. 63–69, Jan. 2000.

[20] Z. Wu, C. Shi, and K. H. Khayat, "Influence of silica fume content on microstructure development and bond to steel fiber in ultra-high strength cement-based materials (UHSC)," *Cement Concrete. Compos.*, vol. 71, pp. 97–109, Aug. 2016.

[21] O. Kele temur, E. Arıcı, S. Yıldız, and B. Gökçer, "Performance evaluation of cement mortars containing marble dust and glass fiber exposed to high temperature by using Taguchi method," *Construct. Building Mater.*, vol. 60, pp. 17–24, Jun. 2014.

[22] A. M. Brandt, "Fibre reinforced cement-based (FRC) composites after over 40 years of development in building and civil engineering," *Compos. Struct.*, vol. 86, nos. 1–3, pp. 3–9, Nov. 2008.

[23] Z. K. Awad, T. Aravinthan, Y. Zhuge, and F. Gonzalez, "A review of optimization techniques used in the design of fibre composite structures for civil engineering applications," *Mater. Des.*, vol. 33, pp. 534–544, Jan. 2012.

[24] H. Saadatmanesh, "Fiber composites for new and existing structures," *ACI. Struct. J.*, vol. 91, no. 3, pp. 346–354, 1994.

[25] N. Cristelo, V. M. C. F. Cunha, M. Dias, A. Gomes, T. Miranda, and N. Araújo, "Influence of discrete fibre reinforcement on the uniaxial compression response and seismic wave velocity of a cement-stabilised sandy-clay," *Geotextiles Geomembranes*, vol. 43, no. 1, pp. 1–13, Feb. 2015.

[26] N. Cristelo, V. M. C. F. Cunha, A. T. Gomes, N. Araújo, T. Miranda, and M. de Lurdes Lopes, "Influence of fibre reinforcement on the post-cracking behaviour of a cement-stabilised sandy-clay subjected to indirect tensile stress," *Constr. Build. Mater.*, vol. 138, pp. 163–173, May 2017.

[27] Y. Cai, B. Shi, C. W. W. Ng, and C.-S. Tang, "Effect of polypropylene fibre and lime admixture on engineering properties of clayey soil," *Eng. Geol.*, vol. 87, pp. 230–240, Nov. 2006.

[28] Y. Yilmaz, "Compaction and strength characteristics of fly ash and fiber amended clayey soil," *Eng. Geol.*, vol. 188, pp. 168–177, Apr. 2015.

[29] A. Hamidi and M. Hooresfand, "Effect of fiber reinforcement on triaxial shear behavior of cement treated sand," *Geotextiles Geomembranes*, vol. 36, pp. 1–9, Feb. 2013.

[30] N. Consoli, M. Bassani, and L. Festugato, "Effect of fiber-reinforcement on the strength of cemented soils," *Geotextiles Geomembranes*, vol. 28, no. 4, pp. 344–351, Aug. 2010.

[31] S. Lirer, A. Flora, and N. Consoli, "On the strength of fibre-reinforced soils," *Soils. Found.*, vol. 51, no. 4, pp. 601–609, 2011.

[32] Y. Wang, P. Guo, S. Shan, H. Yuan, and B. Yuan, "Study on strength influence mechanism of fiber-reinforced expansive soil using jute," *Geotech. Geological Eng.*, vol. 34, no. 4, pp. 1079–1088, Aug. 2016.

[33] X. W. Yi, G. W. Ma, and A. Fourie, "Compressive behaviour of fibre-reinforced cemented paste backfill," *Geotextiles Geomembranes*, vol. 43, no. 3, pp. 207–215, Jun. 2015.

[34] V. Anggraini, A. Asadi, B. B. K. Huat, and H. Nahazanan, "Effects of coir fibers on tensile and compressive strength of lime treated soft soil," *Measurement*, vol. 59, pp. 372–381, Jan. 2015.

[35] G. Barla and N. Innaurato, "Indirect tensile testing of anisotropic rocks," *Rock. Mech.*, vol. 5, no. 4, pp. 215–230, Dec. 1973.

[36] D. W. Hobbs, "The tensile strength of rocks," *Int. J. Rock Mech. Mining Sci. Geomech. Abstr.*, vol. 1, no. 3, pp. 385–396, May 1964.

[37] E. Komurlu, A. Kesimal, and S. Demir, "Experimental and numerical analyses on determination of indirect (splitting) tensile strength of cemented paste backfill materials under different loading apparatus," *Geomech. Eng.*, vol. 10, no. 6, pp. 775–791, Jun. 2016.

[38] X. Chen, X. Shi, J. Zhou, Q. Chen, E. Li, and X. Du, "Compressive behavior and microstructural properties of tailings polypropylene fibre-reinforced cemented paste backfill," *Construct. Building Mater.*, vol. 190, pp. 211–221, Nov. 2018.

[39] M. Wang, X. Shi, J. Zhou, and X. Qiu, "Multi-planar detection optimization algorithm for the interval charging structure of large-diameter longhole blasting design based on rock fragmentation aspects," *Eng. Optim.*, vol. 50, no. 12, pp. 2177–2191, Mar. 2018.

[40] *Standard Practice for Classification of Soils for Engineering Purposes (Unified Soil Classification System)*, Standard ASTM D2487-11, 2011.

[41] R. Nazir, E. Momeni, D. J. Armaghani, and M. F. M. Amin, "Correlation between unconfined compressive strength and indirect tensile strength of limestone rock samples," *Electron. J. Geotech. Eng.*, vol. 18, no. 1, pp. 1737–1746, Jan. 2013.

[42] K. Faizi, D. J. Armaghani, H. Sohaei, A. S. A. Rashid, and R. Nazir, "Deformation model of sand around short piles under pullout test," *Measurement.*, vol. 63, pp. 110–119, Mar. 2015.

[43] *Standard Test Method for Splitting Tensile Strength of Intact Rock Core Specimens*, Standard ASTM D3967-08, 2008.

[44] X. Chen, X. Shi, J. Zhou, X. Du, Q. Chen, and X. Qiu, "Effect of overflow tailings properties on cemented paste backfill," *J. Environ. Manage.*, vol. 235, pp. 133–144, Apr. 2019.

[45] B. Ercikdi, F. Cihangir, A. Kesimal, H. Deveci, and . Alp, "Utilization of industrial waste products as pozzolanic material in cemented paste back-fill of high sulphide mill tailings," *J. Hazard Mater.*, vol. 168, nos. 2–3, pp. 848–856, Sep. 2009.

[46] D. J. Armaghani, E. T. Mohamad, E. Momeni, M. Monjezi, and M. S. Narayanasamy, "Prediction of the strength and elasticity modulus of granite through an expert artificial neural network," *Arabian J. Geosci.*, vol. 9, no. 1, p. 48, Jan. 2016.

[47] D. Armaghani, E. Mohamad, E. Momeni, and M. Narayanasamy, "An adaptive neuro-fuzzy inference system for predicting unconfined compressive strength and Young's modulus: A study on Main Range granite," *Bull. Eng. Geol. Environ.*, vol. 74, no. 4, pp. 1301–1319, Nov. 2015.

[48] Y. Wu, H. Zhao, C. Zhang, L. Wang, and J. Han, "Optimization analysis of structure parameters of steam ejector based on CFD and orthogonal test," *Energy*, vol. 151, pp. 79–93, May 2018.

[49] X. Jia and Q. Ouyang, "Optimal design of point-focusing shear vertical wave electromagnetic ultrasonic transducers based on orthogonal test method," *IEEE. Sens. J.*, vol. 18, no. 19, pp. 8064–8073, Oct. 2018.

[50] X. Zhao, L. Xu, C. Fang, H. Jiang, J. Li, and M. Ouyang, "Study on voltage clamping and self-humidification effects of pem fuel cell system with dual recirculation based on orthogonal test method," *Int. J. Hydrogen Energy*, vol. 43, no. 33, pp. 16268–16278, Aug. 2018.

[51] C. Li and J. G. Zornberg, "Mobilization of reinforcement forces in fiber-reinforced soil," *J. Geotech. Geoenviron. Eng.*, vol. 139, no. 1, pp. 107–115, Jan. 2013.

[52] B. Bing and M. D. Cohen, "Does gypsum formation during sulfate attack on concrete lead to expansion?" *Cement Concrete Res.*, vol. 30, no. 1, pp. 23–117, Jan. 2000.

XIN CHEN received the B.S. and M.S. degrees in mining engineering from Central South University, Changsha, China, where he is currently pursuing the Ph.D. degree. He is also visiting the École Polytechnique de Montréal, Montreal, Canada. He is an author of over 15 papers published in related international conference proceedings and journals, and the holder of six patents. His research interests include cemented paste backfill, fiber materials, tailings disposal, mine ventilation, and CFD simulation. His awards and honors include the National Scholarship for the Ph.D. student.

XIUZHI SHI received the Ph.D. degree in mining engineering from the School of Resources and Safety Engineering, Central South University, Changsha, China, in 2007, where he is currently a Professor. He is an author of over 100 papers published in related international conference proceedings and journals, and the holder of more than 15 patents. His research interests include mine backfill technology, mine blasting technology, and mine safety engineering. He has served as a reviewer of over 15 journals. He received three projects of Provincial/Ministerial Science and Technology Awards. He presided over more than 80 engineering research projects.
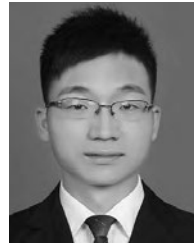
JIAN ZHOU received the Ph.D. degree from the School of Resources and Safety Engineering, Central South University, Changsha, China, in 2015. From 2013 to 2014, he was a Visitor Scholar with McGill University, Montreal, Canada. He is currently an Assistant Professor with the School of Resource and Safety Engineering, Central South University. His current research interests include prediction and control of mining and geotechnical engineering hazards using supervised machine learning methods, including rock burst in deep hard rock mining and high-stress conditions, pillar and slope stability analysis, blast vibration in open pit, and slope stability analysis. He has authored over 60 papers published in related international conference proceedings and journals. He is a member of the ISRM. He has served as a Reviewer of over 20 journals.

ZHI YU received the B.S. and M.S. degrees from the Hunan University of Science and Technology, Xiangtan, China. He is currently pursuing the Ph.D. degree from Central South University, Changsha, China. He has authored three papers published in related international conference proceedings and journals, and is the holder of two patents. His research interests include mine blasting technology and controlled blasting technology.

● ● ●